



# Evolution of microstructure and electrical conductivity of electroless copper deposits on a glass substrate

Xiaoyun Cui, David A. Hutt\*, Paul P. Conway

Wolfson School of Mechanical and Manufacturing Engineering, Loughborough University, Loughborough, LE11 3TU, UK

## ARTICLE INFO

### Article history:

Received 10 November 2011

Received in revised form 22 May 2012

Accepted 24 May 2012

Available online 1 June 2012

### Keywords:

Electroless deposition

Copper

Microstructure

Glass substrate

Deposition rate

Electrical conductivity

Scanning electron microscopy

## ABSTRACT

This paper describes the evolution of the microstructure and conductivity of electroless copper deposition on a glass substrate for applications in electronics manufacture. The glass was activated using a (3-aminopropyl) trimethoxysilane pre-treatment followed by a Pd/Sn catalyst. Surface morphology of the deposited copper films was characterized using a dual beam focused ion beam field emission scanning electron microscope, and together with atomic force microscopy, showed clearly that the roughness and grain size tended to increase with the plating time. Film thickness measurements showed a high initial deposition rate, which slowed to a constant level as the thickness increased above 100 nm. This corresponded with the resistivity of the films which decreased rapidly as the thickness increased from 20 to 100 nm, but then remained largely stable at a level approximately twice that of bulk copper.

© 2012 Elsevier B.V. All rights reserved.

## 1. Introduction

The increasing demands for miniaturisation of electronic products requires a corresponding increase in the number of electrical connections between components per unit area. This is particularly important for the semiconductor devices at the heart of most products, where their increasing functionality is being implemented in ever decreasing package sizes, leading to a very high interconnection density. However, this trend is pushing the current manufacturing methods for Printed Circuit Boards (PCBs) and other substrates, to which the semiconductor devices must be connected, to the limit. Multilayer circuit board design is necessary to fan out the many interconnections from the surface area of the integrated circuits. However, the associated reduction in metal track line widths and pitches results in many drawbacks, such as interconnect resistance and parasitic capacitance, eventually leading to low signal transmission speed. In addition, the fabrication of small diameter vias to interconnect different layers of the substrate becomes problematic due to alignment issues. Significant advances have been achieved in production techniques, however some substrate materials including traditional glass fibre-epoxy composites and flexible substrates, show dimensional instability during manufacture due to changes in humidity and temperature that limit the accurate alignment of features, particularly on multiple layers. Glass sheets are a promising material from which to manufacture high

density substrates as they offer good dimensional stability and coefficient of thermal expansion similar to silicon. In addition, the transparency of glass enables the viewing of buried features for accurate machining, and makes it a promising material for carrying optical signals for future optical interconnect [1,2]. However, to form reliable electrically conductive tracks and reflective mirror surfaces for optical waveguides, stringent demands on the quality of the metallic films deposited onto the glass surfaces are necessary.

Electroless copper deposition has been widely used for high volume manufacture of metallised parts and has established infrastructure within the electronics industry due to its relatively low cost and low processing temperature. Furthermore, it has also been used as an interconnect metallisation in dual-damascene structures of ultra-large scale integrated circuits and in the fabrication of micro-electro mechanical systems [3–5]. Therefore, electroless copper deposition is a promising route to the metallisation of glass for multilayer circuit board interconnection. The deposition of a metallic copper layer onto a glass substrate by electroless plating requires the previous creation of catalytic sites on the glass surface; such catalysts include Ag colloid [6] or PdCl<sub>2</sub> solutions [7], but the most popular catalyst is a Pd/Sn colloid (or Pd–Sn) [8,9]. However, it has been noticed that the adhesion of the Pd/Sn catalyst directly to the smooth glass is poor and therefore a modified pre-treatment or seed layer is required [10,11]. It has been shown that a self-assembled monolayer such as 2-(trimethoxysilyl)ethyl-2-pyridine, (3-aminopropyl)triethoxysilane or 3-(2-aminoethylamino)propyl-trimethoxysilane, can provide a promoting layer of chemical ligand for anchoring Pd based catalysts [12–14]. Some research has reported the microstructure and crystal

\* Corresponding author. Tel.: +44 1509 227658; fax: +44 1509 227648.

E-mail address: [D.A.Hutt@lboro.ac.uk](mailto:D.A.Hutt@lboro.ac.uk) (D.A. Hutt).

structure of electroless copper films deposited on a number of substrate types with Pd based catalysts [10,15,16]. However, there appear to be no detailed reports of the morphology development of electroless copper deposits on glass substrates with a (3-aminopropyl)trimethoxysilane adhesion promotion layer. Therefore, as part of a wider investigation of the adhesion and patterning of electroless copper films on glass for electrical applications [17], in this study the evolution of the deposit morphology, microstructure, grain size and roughness was mainly investigated. In addition, the correlation between electrical conductivity and coating thickness was also addressed as the electrical properties play an important role in copper interconnect applications.

## 2. Experimental section

### 2.1. Materials

CMZ glass sheets (100  $\mu\text{m}$  thick) obtained from Qioptiq were used as substrates in this work. The glass sheet was sliced into rectangular strips of about 3 cm  $\times$  5 cm in size. (3-Aminopropyl)trimethoxysilane (APTS) was purchased from Sigma-Aldrich. Methanol and Decon 90 cleaning agent were obtained from Fisher Scientific, UK. The self-accelerating, formaldehyde-based electroless copper plating solution (Circuposit 4750), pre-dip bath (Circuposit 3340) and Pd/Sn catalyst (Circuposit 3344) were obtained from Rohm and Haas, UK and prepared according to the manufacturer's guidelines.

### 2.2. Electroless copper process

The electroless copper process for deposition on to glass can be divided into five main steps: Decon cleaning, self-assembled monolayer (SAM) deposition, pre-dip, catalyst and electroless copper, as shown in Table 1. After cleaning, the first process step involved the silanisation of the glass by APTS to form a SAM. The APTS molecule ( $\text{NH}_2-(\text{CH}_2)_3-\text{Si}(\text{OCH}_3)_3$ ) consists of a head group ( $-\text{Si}(\text{OCH}_3)_3$ ) that couples to the glass surface forming Si–O bonds, enabling the methylene chains ( $-(\text{CH}_2)_3-$ ) to pack together, thereby exposing the tail group ( $-\text{NH}_2$ ) at the surface, which can interact with the Pd/Sn catalyst particles. After the formation of the SAM, the sample was rinsed with deionized (DI) water, dried and immersed into the pre-dip solution. It was then exposed to the catalyst for the required time and rinsed with DI water. It was observed that without the SAM layer, the catalyst would not adhere to the smooth glass surface and was easily rinsed away, but with the SAM layer, a uniform coverage of catalyst particles was achieved. The electroless copper bath operating with a pH value of 11.5 was a self-accelerating solution that was able to activate the catalyst particles for subsequent plating, for which different immersion times were used to control the copper thickness.

**Table 1**  
Experimental process for electroless copper deposition on glass.

Step	Process	Solution concentration	Time	Temp.
1	Cleaning	Decon 90 (2.67 vol.%) in water	8 h	R.T.
2	Rinse	DI water	3–5 min	R.T.
3	SAM formation	APTS ( $5 \times 10^{-3}$ mol/l) in methanol (95%) and water (5%)	1 h	R.T.
4	Rinse and dry	DI water and air blower	3–5 min	R.T.
5	Pre-dip	Circuposit 3340	1 min	R.T.
6	Catalyst	Circuposit 3344	2 min	R.T.
7	Rinse	DI water	3–5 min	R.T.
8	Electroless copper	Circuposit electroless copper 4750	0–30 min	40 °C
9	Rinse and dry	DI water and air blower	10 min	R.T.

R.T. = room temperature.

### 2.3. Characterization

#### 2.3.1. Morphology

The morphology of deposits on surfaces was observed using a LEO 1530VP field emission scanning electron microscope operating at 5 kV and 30 pA. A Digital Instruments Atomic Force Microscope (AFM) 3000 operating in tapping mode, with Si tip cantilevers of 5–10 nm nominal curvature was used to investigate the copper surface roughness and morphology using the tapping mode at a frequency of 1.0 kHz. The average copper grain sizes were determined by the AFM measurement carried out on an area of  $500 \times 500 \text{ nm}^2$ , and the roughness was represented as an  $R_a$  value determined from a measurement of an area of  $10 \times 10 \mu\text{m}^2$ .

Cross-sections through the copper layers were prepared by using a focused  $\text{Ga}^+$  ion beam operating at 12 pA and 30 kV in a FEI Nova 600 Nanolab microscope. Once the area of interest was selected, it was coated with a Pt film about 400 nm to 1  $\mu\text{m}$  thick in order to protect the surface and a trench was then milled through the sample using the  $\text{Ga}^+$  beam, ready for subsequent scanning electron microscope (SEM) imaging. The copper film thickness was determined using the system accessory software.

#### 2.3.2. Electrical properties

The resistivity of the electroless copper films was measured using four-point Au probes attached to a Keithley 580 micro-ohmmeter. The probes were positioned in a line on the sample surface with a pitch of 2 mm. Each data point was collected from samples with an average value taken from a total of 10 different measurements on each sample.

## 3. Results and discussion

### 3.1. Morphology of electroless copper deposits

It was noticed that both SAM pre-treatment and catalyst activation are essential to achieve good adhesion and improved coverage of the copper coating. Therefore, in the following section all results were obtained from samples prepared using these treatments as described earlier in Table 1. These parameters, including APTS and catalyst immersion time, and electroless copper plating bath parameters were determined by investigating a range of values that led to the best coverage and adhesion of the copper to the glass. With these parameters, uniform coatings of copper were routinely achieved. The adhesion of these layers has been discussed elsewhere [18], but in summary, it was found that up to ~150 nm thickness, the coatings adhered well to the glass and could not be removed using a tape test, however thicker coatings showed reduced adhesion and could be peeled away.

Morphological investigation of the electroless copper as a function of deposition time was carried out to characterize how the coating developed. Fig. 1 shows SEM and corresponding AFM images of electroless copper deposits on glass for different plating times. For very short plating times (e.g. 0.5 min), the surface was found to be smooth and there were no obvious copper particles. More particles appeared on the surface when the plating time was increased to 1 min, for which the average copper grain size was 48 nm with a narrow size distribution. The grain size gradually increased with the plating time such that after 3 min, copper particles were found to be in the range of 70–80 nm. At this stage the film appeared to be uniform and continuous across the surface. After 5 min deposition, the copper particles had grown larger and become polygonal in shape. The roughness of the corresponding deposited copper was determined directly from the AFM images using the system software. As the copper thickness increased from 52 nm to 175 nm, the roughness increased from 6.4 nm to 12.6 nm. Meanwhile, there was an overall increase of the grain size with increasing thickness. For continuous films, it is

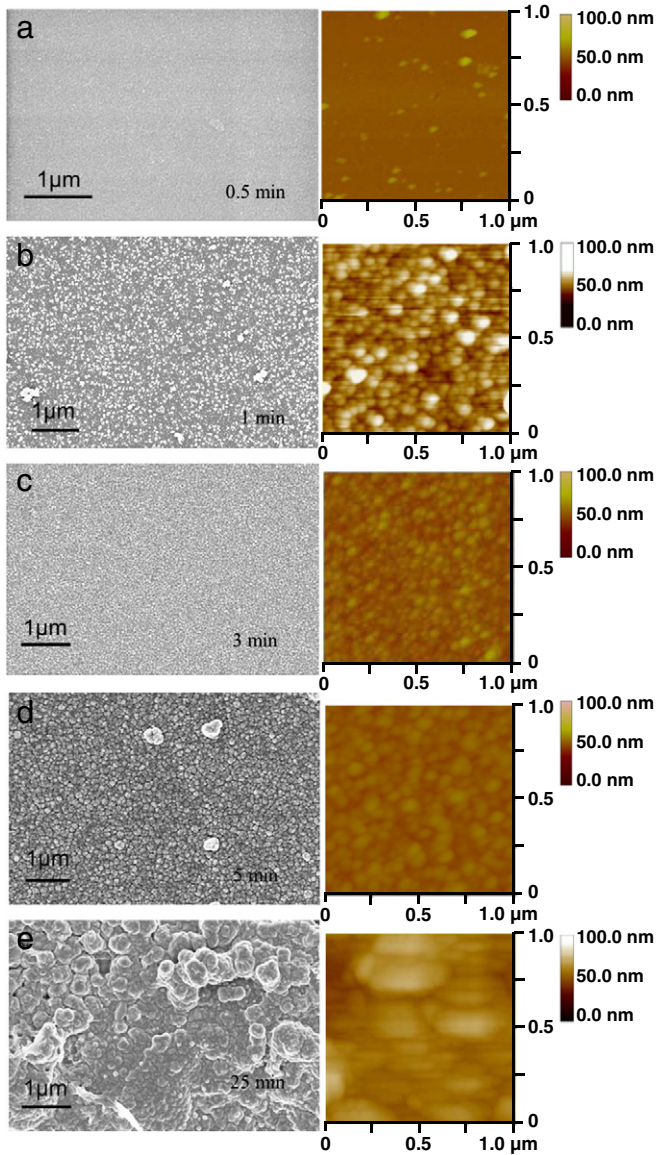


**Fig. 1.** SEM and corresponding AFM images of electroless copper deposits on glass for different plating times: (a) 0.5 min, (b) 1 min, (c) 3 min, (d) 5 min and (e) 25 min.

expected that the roughness of the deposit surfaces would increase along with the plating time due to grain growth, which is in good agreement with many other observations [19].

The microstructure evolution of the electroless copper grown on the APTS pre-treated glass substrate is directed by the Pd–Sn catalyst particles. Therefore, the main mechanism shown here is thought to be grain growth of copper particles initially formed around the Pd–Sn catalyst particles and coalescence of small islands or clusters, then the islands increase in size until they impinge on each other to form a continuous film. This film growth results in less grain boundaries appearing along with the increase in plating time. A schematic diagram of the copper film formation using electroless deposition is shown in Fig. 2, which is analogous to the Volmer–Weber mode for physical vapour deposition [20]. Others have suggested that the catalyst particles may be mobile on a plain glass substrate due to weak physical interactions [16] and that this can lead to coalescence and grain growth, however in the present study, the SAM layer is likely to improve the strength of bonding between the Pd catalyst and the glass so that particle movement would not be expected to take place readily.

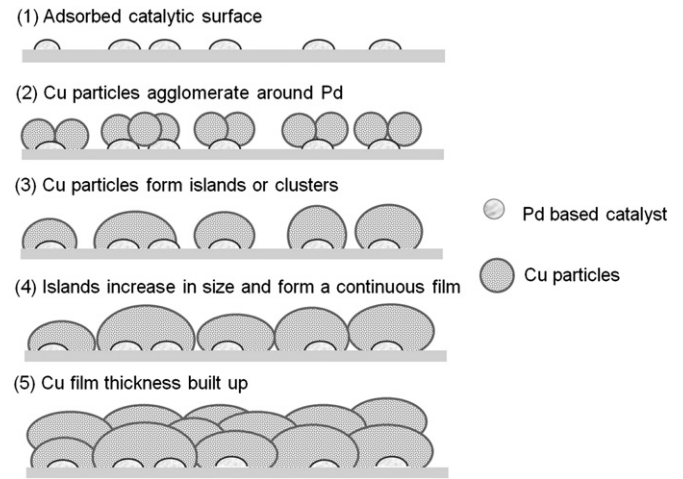


**Fig. 2.** Schematic diagram of Cu film growth in electroless deposition.

SEM micrographs of the electroless copper deposits at 5 min, 10 min and 25 min plating time are shown in Fig. 3. The cross-sections were prepared using focused ion beam (FIB) machining and the micrographs show clearly the Pt layer deposited first as

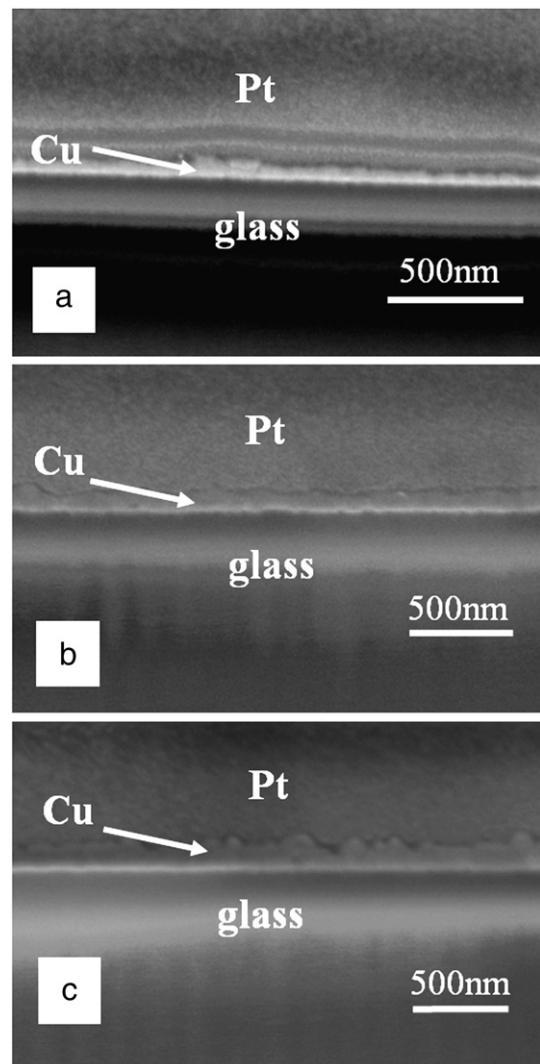


**Fig. 3.** SEM micrographs of FIB machined cross-sections of electroless copper deposited for different times at 40 °C: (a) 5 min, (b) 10 min and (c) 25 min.



protection prior to FIB machining and the Cu layer and glass substrate. It is apparent that the copper thicknesses increased with the electroless plating time. The thickness was measured using the system software from eight different points and the final average values obtained as  $52 \pm 9$  nm,  $92 \pm 12$  nm and  $175 \pm 18$  nm, for 5, 10 and 25 min respectively. Meanwhile, it can be observed that all three thin films were continuous along the glass surface, although deposits prepared for 5 min and 10 min were less rough than the film formed at 25 min in agreement with the SEM images and the AFM measurements of Fig. 1. It was noted that there were no obvious voids observed in the coatings indicating that the low deposition rate leads to good coverage.

### 3.2. Deposition rate

The electroless copper deposition thickness as a function of plating time in the solution at different operating temperature was explored over the range of room temperature to  $55^\circ\text{C}$ . It was very difficult to start the deposition below  $30^\circ\text{C}$ , and it was also found that the adhesion between electroless copper deposits and glass became weak once the plating bath temperature was above  $50^\circ\text{C}$  due to rapid reaction, which also highlights that temperature has a strong effect on deposition rates. Therefore, to balance thickness and adhesion strength,  $40^\circ\text{C}$  was chosen for the following study. Fig. 4 shows the copper thickness with deposition time at  $40^\circ\text{C}$ . It was seen that the practical deposition rate on the glass substrate measured here is fairly low, only approximately 200 nm thick in 30 min, which is close to the deposition rate reported by Dubin [21] for electroless copper deposition on a Si wafer surface at  $40^\circ\text{C}$ . It was reported that a deposition rate of  $18\ \mu\text{m/h}$ , albeit at  $70^\circ\text{C}$ , can be achieved on polymer surfaces using a different electroless copper bath [22]. To demonstrate the influence of substrate on electroless deposition rate, FR4 PCB material was also plated in the current study using the same conditions and the deposit thickness built to  $1.7\ \mu\text{m}$  in 30 min. Clearly, the deposition rate varied greatly with the different substrates, not just because of different temperature, pH value and bath compositions which have been characterized by other research. This observation could be partly supported by Donahue's [23] kinetics research on electroless copper plating and Nakahara's [16] electroless Cu microstructure investigations on different substrates, including metals and non-metallic materials, in which they showed that the substrate plays a role in affecting the formation of nuclei. They attributed the varied deposition rate to the different catalytic properties of the substrate surface on which the deposition occurs. In this study it appears more difficult to create effective nucleation sites on glass compared with the more porous FR4 substrate surface.

As for Fig. 4, it was noted that the copper deposition rate was not constant at  $40^\circ\text{C}$ . It was seen that the deposition rate of the first 3 min was higher and slowed down, so that after around 10 min the

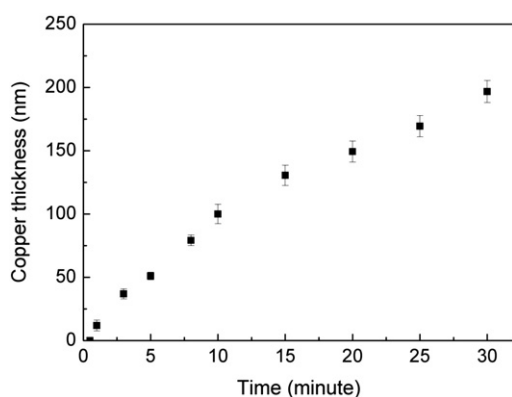


Fig. 4. Copper thickness as a function of deposition time at  $40^\circ\text{C}$ .

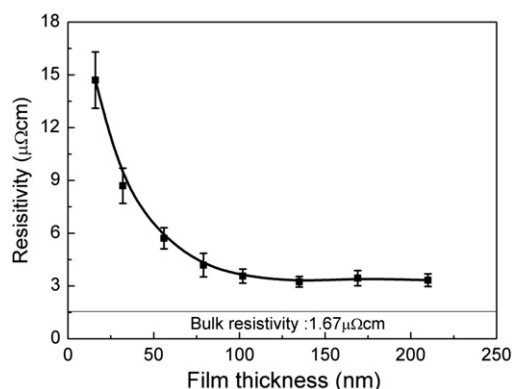


Fig. 5. Copper resistivity as a function of film thickness, d.

plating rate became steady with an almost linear increase in deposit thickness with plating time from 10 min to 30 min. The corresponding average growth rates were around 10 nm/min and 6 nm/min up to and after 10 min respectively. These different deposition rates were called the “initial” and “final” rates discussed by Dumesic and co-workers [24], which also suggested that the initial rate was usually larger than the final rate, likely due to different catalytic effects. They suggested that the change in deposition rate could be related to the coverage of the catalyst particles. It has also been noted [25] that the time for the initial Cu particles to grow on a catalytic Pd core is very prompt, while the subsequent expansion of the Cu islands to merge together takes longer. Referring again to the model of Fig. 2, when the reaction started, the catalytic surfaces could offer enough nucleation sites for cupric ions to react, resulting in a higher deposition speed. Later, the nucleation sites were largely covered by copper particles which grew and coalesced so the deposition rate went down. In the present study, a continuous copper film appeared after 3 min deposition which corresponded with the change in plating rate. In addition to catalytic effects, the deposits may also have different initial morphologies compared to later on, which could also affect the plating rate.

### 3.3. Electrical properties of electroless copper deposits

The resistivity of the copper films as a function of the film thickness prepared at  $40^\circ\text{C}$  is presented in Fig. 5. It is clear that the resistivity of copper thinner than 17 nm (1 min deposition) was very high and that it decreased sharply with increasing thickness. The high resistivity of ultra-thin copper films is thought to occur because of discontinuities between the small islands on the surface [26] leading to a limited number of electrical pathways for conduction (step 3 in Fig. 2). With the film becoming thicker, the copper islands begin to grow and coalesce, increasing the number of contacts between previously isolated islands (step 4 in Fig. 2). As a result, there is a rapid increase in the electron mobility from one island to another, thereby decreasing the film resistivity. The resistivity was almost constant at  $3.5\ \mu\Omega\text{cm}$  if the copper thickness was over 100 nm ( $>10$  min deposition). The levelling out of the resistivity with thickness at around 80 to 100 nm also corresponded with the change in plating rate observed earlier in Fig. 4. Though the plateau value of resistivity is two times that of pure bulk copper ( $1.67\ \mu\Omega\text{cm}$ ), comparing this resistivity with the much larger values of  $300\ \mu\Omega\text{cm}$  [27] and  $12\ \mu\Omega\text{cm}$  [28] reported for a 150 nm electroless copper film formed on an  $\text{NH}_2$ -SAM treated silicon surface and 100 nm electroless copper film obtained on a SH-SAM treated polyethylene terephthalate surface, it can be concluded that the electroless copper film deposited here had better electrical properties. It was reported that the electrical resistivity of copper films decreased from  $6.23\ \mu\Omega\text{cm}$  to  $3.3\ \mu\Omega\text{cm}$  with increasing annealing time up to 90 min at  $200^\circ\text{C}$  [10], which was attributed to the reduction in defects and the number of grain boundaries in the film. For comparison, in the present study, resistivity

measurements were carried out on a few samples annealed in a vacuum oven at  $180\text{ }^{\circ}\text{C} \pm 3\text{ }^{\circ}\text{C}$  for 1 h, however no decrease of resistivity was observed. Zhu et al. [27] supposed that the relatively high resistivity was due to poor connectivity between copper particles, while other evidence presented the reason for low conductivity as due to the polycrystalline copper film with small grains and many grain boundaries that scatter electrons, thus reducing the conductivity [28]. Accordingly, to obtain good conductivity of the copper film, it is necessary to slow down the rate of crystal nucleation and to accelerate grain growth and hence decrease the number of grain boundaries. It has already been shown that the deposition rate in this study is low, which is not good for volume production in industry, but the much denser films without many grain boundaries and defects lead to relatively low resistivity. It was also noticed that the resistivity levels obtained here are very close to copper films prepared by ion beam deposition [29], which is often considered to provide one of the best quality film conductivities.

#### 4. Conclusions

The evolution of the microstructure and electrical conductivity of electroless copper films on glass was investigated as a function of deposit thickness. Electroless copper films with good surface morphology and conductivity were obtained on transparent glass substrates by means of a self-assembled monolayer that acted as an adhesion promotion layer to ensure the attachment of the Pd/Sn catalyst. Metallographic studies of the electroless copper deposits revealed that their topographic structures showed uniform and fine particle distribution. The electrical resistivity of electroless copper films decreased with increasing thickness and a constant  $3.5\text{ }\mu\Omega\text{ cm}$  was obtained on or above 100 nm thickness. The results indicated that a crucial step of the deposition process with respect to microstructure and conductivity is the initial growth of the metallic copper film onto catalytic nucleation sites.

#### Acknowledgments

The authors would like to thank the EPSRC for financial support through the Innovative Electronics Manufacturing Research Centre and are grateful to Qioptiq for technical support.

#### References

- [1] H. Schröder, N. Arndt-Staufenbiel, A. Beier, F. Ebling, M. Franke, E. Griesse, S. Intemann, J. Kostelnik, T. Kühler, R. Mödinger, I. Roda, I. Schlosser, 58th Electronic Components and Technology Conference, Florida, U.S.A., May 27–30, 2008, p. 268.
- [2] L. Brusberg, H. Schröder, M. Töpfer, N. Arndt-Staufenbiel, J. Röder, M. Lutz, H. Reichl, 59th Electronic Components and Technology Conference, San Diego, U.S.A., May 26–29, 2009, p. 207.
- [3] S.Y. Chang, C.W. Lin, H.H. Hsu, J.H. Fang, S.J. Lin, J. Electrochem. Soc. 151 (2004) C81.
- [4] S.P. Murarka, R.J. Gutmann, A.E. Kaloyeros, W.A. Lanford, Thin Solid Films 236 (1993) 257.
- [5] Y. Shacham-Diamand, A. Inberg, Y. Sverdlov, V. Bogush, N. Croitoru, H. Moscovich, A. Freeman, Electrochim. Acta 48 (2003) 2987.
- [6] Z. Liu, Q. He, P. Hou, P. Xiao, N. He, Z. Lu, Colloids Surf. A 257/258 (2005) 283.
- [7] M. Charbonnier, M. Romand, Surf. Coat. Technol. 162 (2003) 19.
- [8] B.J. Meenan, N.M.D. Brown, J.W. Wilson, Appl. Surf. Sci. 74 (1994) 221.
- [9] J. Zhao, R. Tian, J. Zhi, Appl. Surf. Sci. 254 (2008) 3282.
- [10] R.K. Aithal, S. Yenamandra, R.A. Gunasekaran, P. Coane, K. Varahramyan, Mater. Chem. Phys. 98 (2006) 95.
- [11] Y.J. Chen, E.T. Kang, K.G. Neoh, W. Huang, Langmuir 17 (2001) 7425.
- [12] W.J. Dressick, C.S. Dulcey, J.H. Georger, G.S. Calabrese, J.M. Calvert, J. Electrochem. Soc. 141 (1994) 210.
- [13] L. Xu, J. Liao, L. Huang, D. Ou, Z. Guo, H. Zhang, C. Ge, N. Gu, J. Liu, Thin Solid Films 434 (2003) 121.
- [14] E. Delamarche, J. Vichiconti, S.A. Hall, M. Geissler, W. Graham, B. Michel, R. Nunes, Langmuir 19 (2003) 6567.
- [15] Y.S. Kim, J. Shin, J.H. Cho, A. Gregory, E. Ten, D.L. Liu, S. Pimanpang, T.M. Lu, J.J. Senkevich, H.S. Shin, Surf. Coat. Technol. 200 (2006) 5760.
- [16] S. Nakahara, Y. Okinaka, Annu. Rev. Mater. Sci. 21 (1991) 93.
- [17] X.Y. Cui, D. Bhatt, F. Khoshnaw, D.A. Hutt, P.P. Conway, 10th Electronics Packaging Technology Conference, Singapore, Dec 09–12, 2008, p. 12.
- [18] X.Y. Cui, D.A. Hutt, P.P. Conway, 2nd Electronics System-Integration Technology Conference, Greenwich, U.K., Sep 01–04, 2008, Proceedings, 1/2, 1998, p. 105.
- [19] S.T. Shiue, C.H. Yang, R.S. Chu, T.J. Yang, Thin Solid Films 485 (2005) 169.
- [20] A. Wagendristel, Y. Wang, An Introduction to Physics and Technology of Thin Films, World Scientific, Singapore, 1994.
- [21] V.M. Dubin, Y. Shacham-Diamand, B. Zhao, P.K. Vasudev, C.H. Ting, J. Electrochem. Soc. 144 (1997) 898.
- [22] J. Li, H. Hayden, P.A. Kohl, Electrochim. Acta 49 (2004) 1789.
- [23] F.M. Donahue, K.L.M. Wong, R. Bhalla, J. Electrochem. Soc. 127 (1980) 2340.
- [24] J. Dumesic, J.A. Koutsky, T.W. Chapman, J. Electrochem. Soc. 121 (1974) 1405.
- [25] S. Nakahara, C.Y. Mak, Y. Okinaka, J. Electrochem. Soc. 140 (1993) 533.
- [26] H.D. Liu, Y.P. Zhao, G. Ramanath, S.P. Murarka, G.C. Wang, Thin Solid Films 384 (2001) 151.
- [27] P.X. Zhu, Y. Masuda, K. Koumoto, J. Mater. Chem. 14 (2004) 976.
- [28] S. Sawada, Y. Masuda, P.X. Zhu, K. Koumoto, Langmuir 22 (2006) 332.
- [29] J.W. Lim, K. Mimura, M. Isshiki, Appl. Surf. Sci. 217 (2003) 95.